

Combining the advantages of superconducting MgB_2 and CaC_6 in one material: Suggestions from first-principles calculations

Amy Y. Liu¹ and I. I. Mazin^{1,2}¹*Department of Physics, Georgetown University, Washington, DC 20057-0995, USA*²*Center for Computational Materials Science, Naval Research Laboratory, Washington, DC 20375, USA*

(Received 8 January 2007; published 23 February 2007)

We show that a recently predicted layered phase of lithium monoboride Li_2B_2 combines the key mechanism for strong electron-phonon coupling in MgB_2 (i.e., interaction of covalent B σ bands with B bond-stretching modes) with the dominant coupling mechanism in CaC_6 (i.e., interaction of free-electron-like interlayer states with soft intercalant modes). Yet, surprisingly, the electron-phonon coupling in Li_2B_2 is calculated to be weaker than in either MgB_2 or CaC_6 . We demonstrate that this is due to the accidental absence of B π states at the Fermi level in Li_2B_2 . In MgB_2 , the π electrons play an indirect but important role in strengthening the coupling of σ electrons. Doping Li_2B_2 to restore π electrons at the Fermi level is expected to lead to a new superconductor that could surpass MgB_2 in T_c .

DOI: [10.1103/PhysRevB.75.064510](https://doi.org/10.1103/PhysRevB.75.064510)

PACS number(s): 74.25.Jb, 74.25.Kc, 74.70.Ad

I. INTRODUCTION

The discovery of superconductivity in MgB_2 at $T_c = 39$ K led to a new paradigm for achieving high critical temperatures in conventional superconductors, namely, strong electron-phonon coupling due to metallization of strong covalent bonds.¹ In MgB_2 , this is achieved through the interaction of electrons forming covalent B-B bonds in the graphenelike layers with vibrational modes that stretch and compress these bonds.² Unfortunately, efforts to find related materials with even higher T_c have not been fruitful. This is basically because the electronic states that form the covalent bonds in MgB_2 are quasi-two-dimensional, which makes it difficult to enhance their density of states and their coupling to phonons through simple doping.³ Significant progress may only be possible through the introduction of different types of electronic states at the Fermi level.³

The recent discovery of superconductivity in CaC_6 at $T_c = 11.5$ K,⁴ the highest critical temperature among graphite intercalation compounds (GICs), offers an alternative path to increasing T_c . Although CaC_6 is structurally similar to MgB_2 , it appears that the key electrons and phonons responsible for its superconductivity are distinct from those in MgB_2 .^{5,6} In particular, free-electron-like states that are concentrated in the region between graphene layers dominate the electron-phonon interaction through coupling with soft intercalant modes and with bond-bending modes of the graphene sheet. Incipient lattice instabilities associated with the soft intercalant phonon modes, however, may present obstacles to attaining significantly higher T_c in GICs.^{7,5}

It is intriguing to ask whether the MgB_2 and CaC_6 mechanisms for strong electron-phonon coupling can be incorporated into a single compound to create a superconductor with the potential to surpass MgB_2 . Although neither MgB_2 nor CaC_6 can be easily modified so as to incorporate the key electronic and phonon players from the other material, we show here that it is indeed possible to combine the MgB_2 and CaC_6 paradigms in a different material. Such a material has a good chance of exceeding both MgB_2 and CaC_6 in terms of T_c .

The material of interest is a hypothetical layered form of lithium monoboride Li_2B_2 that recent calculations have predicted to be competitive in energy with known LiB phases.^{8,9} The B graphene sheets in Li_2B_2 are nearly identical to those in MgB_2 . At the Fermi level, there are σ bands derived from B p_{xy} orbitals that form covalent bonds within the layers, as in MgB_2 , and there are interlayer free-electron-like bands, which we shall call ζ bands, as in CaC_6 . By accident, the B p_z -derived π states that are present in both MgB_2 and CaC_6 are missing at the Fermi level in Li_2B_2 . Based on the similarity of the in-plane B physics with MgB_2 , Kolmogorov and Curtarolo have suggested that this material could be a good superconductor in the mold of MgB_2 .⁸

In this paper, we analyze the electronic structure of Li_2B_2 and show that the electron-phonon interaction has sizable contributions not only from the σ bands that dominate the coupling in MgB_2 , but also from the interlayer ζ bands, which are the key players in CaC_6 . Surprisingly, the total electron-phonon coupling in Li_2B_2 is found to be weaker than in either of the other two materials. We show that this is precisely because of the missing π electrons at the Fermi level. Though the π bands in MgB_2 and CaC_6 give only moderate contributions to the electron-phonon coupling, π electrons can indirectly strengthen the coupling of σ electrons with B bond-stretching phonon modes through screening. Doping Li_2B_2 to add π sheets to the Fermi surface would enhance the σ contribution to the electron-phonon coupling, as well as add a modest π contribution. While a relatively low T_c is predicted for pristine Li_2B_2 , an appropriately doped material could have a T_c higher than even MgB_2 .

II. CALCULATIONAL METHODS

Our analysis is based on density functional calculations. The electronic structure was calculated using the WIEN2K general potential linear augmented plane-wave (LAPW) code,¹⁰ with the generalized gradient approximation (GGA) functional in the Perdew-Burke-Ernzerhof form.¹¹ Local orbitals were added to relax the remaining linearization error and APW orbitals were used to improve the convergence

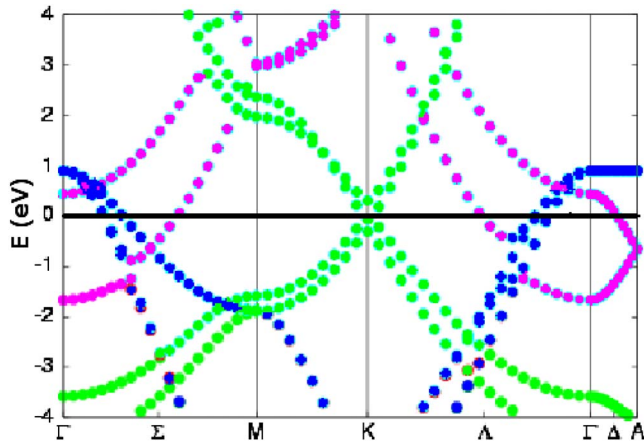


FIG. 1. (Color online) Li_2B_2 band structure near the Fermi level ($E_F=0$). The σ , π , and ζ bands are plotted with blue (black), green (dark gray), and magenta (light gray) symbols, respectively. Note that in the directions plotted, the π bands (green or dark gray) cross the Fermi level only at the K point.

with respect to the cutoff parameter RK_{max} . In most calculations $RK_{\text{max}}=7$ was used, except for the convergence tests with $RK_{\text{max}}=8$. Up to 918 irreducible \mathbf{k} points were used ($32 \times 36 \times 16$). The phonon spectrum and electron-phonon coupling functions were calculated using the linear-response method¹² within the local density approximation. Norm-conserving pseudopotentials¹³ were used, with a plane-wave cutoff of 50 Ry. The dynamical matrix was calculated on a grid of $6 \times 6 \times 2$ phonon wave vectors \mathbf{q} in the Brillouin zone and Fourier interpolated to denser meshes for calculation of the phonon density of states (DOS). For calculation of the electron-phonon matrix elements, the electronic states were sampled on grids of $36 \times 36 \times 12$ \mathbf{k} points in the Brillouin zone.

III. RESULTS AND DISCUSSION

The structure of the hypothetical layered compound Li_2B_2 , first proposed in Ref. 8 (in which it is called MS2), consists of honeycomb B sheets, each surrounded above and below by layers of Li on a triangular lattice. There is a horizontal shift between neighboring Li-B-Li sandwich units, leading to an ABAB... stacking sequence of the Li-B-Li trilayer units. While we find that the optimized structural parameters, particularly the interlayer distances, are sensitive to the details of the electron-ion potential and to the exchange-correlation functional, the band structures calculated within the different approximations are very similar. For the results presented here, we have fixed the structural parameters to the optimized values reported in Ref. 8.

The band structure of Li_2B_2 near the Fermi level is shown in Fig. 1. As expected, the σ (blue) and π (green) states are derived primarily from in-plane B $p_{x,y}$ and out-of-plane B p_z orbitals, respectively. The ζ bands (magenta) have substantial Li sp and B p_z character. The charge density of the ζ electrons, plotted in Fig. 2, is concentrated in the region between Li-B-Li trilayer units, though hybridization with B p_z orbitals is evident. This is similar to the character of ζ bands in

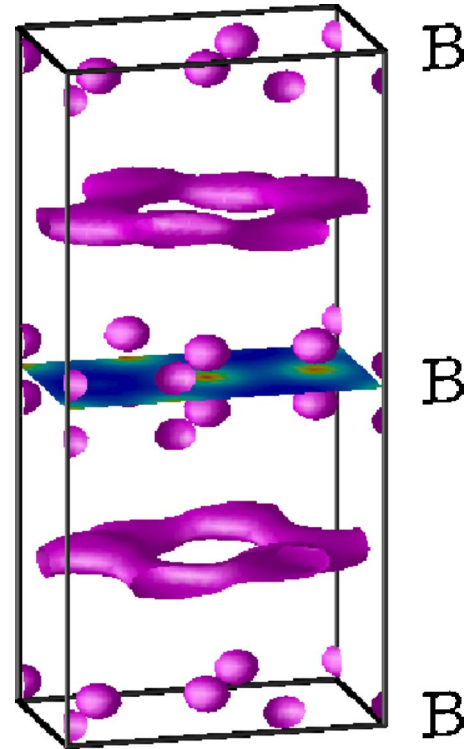


FIG. 2. (Color online) Isosurface of Li_2B_2 charge density corresponding to the ζ state near the Fermi level, halfway between the Γ and A points. The top, center, and bottom planes in the figure contain honeycomb sheets of B. The charge density in the center B plane is shown. Two Li layers lie between each pair of B sheets. The ζ states are primarily concentrated in the interlayer region, but have some B p_z character as well.

GICs.^{5,14,15} The Fermi level in Li_2B_2 lies at the crossing of the π and π^* bands at K, reminiscent of pure graphite. Note, however, that in graphite, the coincidence of the Fermi level with the π - π^* crossing is mandated by the absence of other bands near E_F , while in Li_2B_2 it is accidental. (Expanding c/a by $\sim 10\%$, for example, moves the π - π^* crossing away from the Fermi level by more than 0.5 eV.) Compared to pure graphite, the presence of Li atoms between the B-based graphene sheets (i) makes the π bands more three-dimensional (3D) and lowers their energy relative to the σ bands, and (ii) lowers the ζ bands due to the attractive ionic potential in the interlayer region where the electronic charge in the ζ bands is concentrated.^{6,14} With these relative shifts in the bands, the σ bands, which are completely filled in pure graphite, become partially occupied in Li_2B_2 , while the ζ bands, which are unoccupied in graphite, cross the Fermi level in Li_2B_2 . Hence Li_2B_2 can be viewed as a self-doped analog to pure graphite, with holes in the σ bands exactly compensated by electrons in the ζ band. In contrast, in CaC_6 the π^* band is partially occupied as well.

In comparing the band structures of Li_2B_2 and MgB_2 , which both have B honeycomb sheets separated by “intercalant” layers that donate one electron per B site, key differences in the relative energies of the different types of bands can be attributed to the difference in the separation between B layers. With two Li layers between B sheets in Li_2B_2 , the

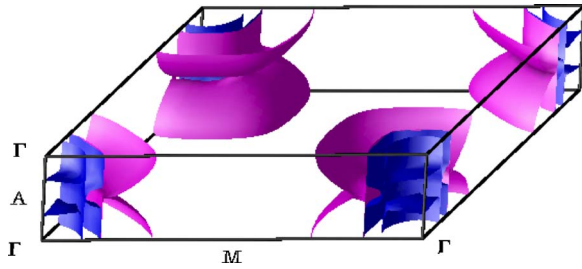


FIG. 3. (Color online) Fermi surface of Li_2B_2 . The cylindrical sheets centered on the Γ -A line arise from the 2D σ bands, while the ellipsoids are due to free-electron-like ζ bands.

B-B interlayer distance in Li_2B_2 (5.4 Å) is significantly larger than in MgB_2 (3.5 Å). This makes the p_{xy} -derived σ bands more 2D in Li_2B_2 , but has little effect on their in-plane dispersion. As in MgB_2 , these bands give rise to nearly cylindrical hole sheets of the Fermi surface surrounding the Γ to A line. As can be seen in the Fermi surface plotted in Fig. 3, there are two nearly degenerate pairs of σ cylinders. The larger separation between B planes also causes the B p_z -derived π bands to be more 2D in Li_2B_2 and raises them in energy so that the π^* band that is partially occupied in MgB_2 becomes unoccupied (and just touches E_F at certain points in the Brillouin zone). The Fermi surface due to the π bands thus disappears in Li_2B_2 . On the other hand, the free-electron-like ζ bands, which are unoccupied in MgB_2 , drop in energy when the interlayer distance is increased since there is a larger interlayer volume available for the electrons to occupy.^{6,16} In Li_2B_2 , the ζ bands produce a slightly squashed ellipsoidal Fermi surface around Γ , with a smaller effective mass for motion along the z direction than in the plane. These ellipsoids are huge compared to the small ζ balls in the CaC_6 Fermi surface,⁶ even though CaC_6 has the most occupied ζ band among all GICs.¹⁴

The topological simplicity of the Fermi surface of MgB_2 , in which sheets of the Fermi surface corresponding to bands of different character are widely separated in reciprocal space, is lost in Li_2B_2 . Not only do the ζ ellipsoids cross all four σ cylinders, they also cross each other. At all of these crossings, there is only weak hybridization between the bands. The multiple crossings between sheets of the Fermi surface arising from bands of different character, along with the presence of bands that nearly touch the Fermi level, make Brillouin-zone integrations sensitive to \mathbf{k} -point sampling. This is especially an issue for calculations of the electron-phonon coupling constants, which involve double integrals over the Fermi surface. The quantitative electron-phonon coupling results presented here likely have larger uncertainties than usual but this does not affect the qualitative picture that emerges.

The phonon density of states $F(\omega)$ and electron-phonon spectral function $\alpha^2F(\omega)$ calculated for Li_2B_2 are shown in Fig. 4. The E_{2g} in-plane bond-stretching B modes that are the key players in superconductivity of MgB_2 are also important in Li_2B_2 , as indicated by the peak in the spectral function near 80 meV. In both materials, these vibrational modes couple strongly to the B σ bands. Given the similarity of the B in-plane physics in the two materials, one expects similar

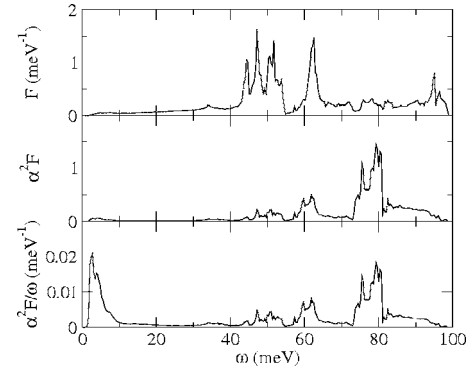


FIG. 4. Li_2B_2 phonon density of states $F(\omega)$, electron-phonon spectral function $\alpha^2F(\omega)$, and ratio of α^2F to frequency ω . The electron-phonon coupling constant λ , which is proportional to the inverse frequency moment of α^2F , has significant contributions from both low-frequency and high-frequency modes.

deformation potentials for the E_{2g} modes.⁸ Indeed, our frozen-phonon calculations using LAPW GGA produce exactly the same deformation potential at Γ : a displacement u opens a gap $\Delta\varepsilon$ such that $\Delta\varepsilon/u=26$ eV/Å, precisely the same as found for MgB_2 .¹ Furthermore, while it is difficult to separate the electronic DOS in Li_2B_2 into contributions from different bands, as is routinely done in MgB_2 , the effective masses derived from the dispersion of the σ bands are within 10% of those in MgB_2 (the heavy band is 9% heavier and the light band 8% lighter). If the phonon frequencies were the same, one would then expect the net interband electron-phonon coupling constant for the σ bands, $\lambda_{\sigma\sigma}$, to be practically the same as in MgB_2 . Surprisingly, the phonon frequencies differ considerably. At the zone center, the E_{2g} phonon frequency of 81 meV in Li_2B_2 is significantly higher than the corresponding 67 meV in MgB_2 ,^{2,17} which likely reduces $\lambda_{\sigma\sigma}$ from ≈ 1 to $\approx 0.6-0.7$.

The hardening of the in-plane B bond-stretching modes in Li_2B_2 is related to the loss of π electrons at the Fermi level. The same electron-phonon coupling process that gives rise to superconductivity also leads to electronic screening of phonons. For a zone-center phonon mode, the softening due to screening by metallic electrons is given by

$$\Delta\omega^2 = -4\omega\langle g^2 \rangle N(0), \quad (1)$$

where $\langle g^2 \rangle$ is a Fermi-surface average of the square of the electron-phonon matrix element g , and $N(0)$ is the electronic DOS at the Fermi level.^{2,18} Because the matrix element g contains a factor of $1/\sqrt{\omega}$, the right-hand side of Eq. (1) is independent of the phonon frequency ω . In MgB_2 , both the σ and π electrons participate in screening the bare E_{2g} phonons. For the E_{2g} mode in MgB_2 , it has been estimated that ω^2 is reduced by about 1500 meV^2 due to screening by π electrons, and by about 2000 meV^2 due to screening by σ electrons, and that the unscreened frequency is $\omega_0 \approx 90$ meV.² In Li_2B_2 , the unscreened frequency and the softening due to σ bands should have roughly the same magnitude as in MgB_2 , which gives a rough estimate for the screened E_{2g} phonon frequency of $\omega = \sqrt{\omega_0^2 - (\Delta\omega^2)_\sigma} \approx 78$ meV. This is consistent with our actual calculations for

Li_2B_2 , which yield a frequency of 81 meV at the zone center. Since only phonons with $q_{xy} < 2k_F^\sigma$, where k_F^σ is the radius of the cylindrical σ sheets of the Fermi surface, can couple to σ electrons, softening by σ electrons is significant only when the in-plane component of the phonon wave vector is less than $2k_F^\sigma$. Indeed, at the zone boundary, our calculations yield a frequency of 92 meV for the lowest E_{2g} branch, consistent with estimates for the unscreened E_{2g} frequency. While Li_2B_2 also has ζ electrons, which are not present in MgB_2 , these are largely localized in the interlayer region and do not couple strongly with the B bond-stretching modes, so they are less effective in screening the E_{2g} phonons. The harder E_{2g} frequencies in Li_2B_2 compared to MgB_2 can thus be attributed to the absence of screening by π electrons.

In addition to the high-frequency E_{2g} peak in the spectral function, there is a low-frequency peak in α^2F arising from ultrasoft modes that involve rigid shifts of the B planes in the z direction coupled with both in-plane and out-of-plane motion of the Li atoms. The frequency of these ultrasoft modes is sensitive to calculational details, so at Γ , for example, the harmonic frequency of about 8 meV obtained in our local density approximation linear-response calculation is somewhat lower than the estimate of 11 meV based on force-constant methods using PAW GGA calculations.⁸ In any case, these low-frequency normal modes couple with the ζ bands, similar to the situation in CaC_6 , where Ca sliding modes interact strongly with interlayer electrons. Although relatively small, the low-frequency peak in α^2F gives a similar contribution to the isotropic electron-phonon coupling constant $\lambda = 2 \int d\omega \alpha^2F/\omega$ as the high-frequency peak (see Fig. 4, bottom panel). The total λ is calculated to be 0.57, with the low-frequency peak contributing about 0.15, and the E_{2g} peak contributing about 0.2. The logarithmically averaged phonon frequency of $\omega_{ln} = \exp[\lambda^{-1} \int d\omega \ln(\omega) \alpha^2F(\omega)/\omega] = 39$ meV, is well below the average frequency of $\omega_{av} = 59$ meV, reflecting the importance of the ultrasoft modes.

From the point of view of T_c , the prospects for Li_2B_2 do not look optimistic compared to MgB_2 , because of both the lack of a π -band contribution to λ , and, perhaps more importantly, the hardening of the key E_{2g} phonons that are no longer screened by π electrons. Neglecting possible multi-band effects and using the McMillan equation¹⁹ with a typical Coulomb parameter of $\mu^* = 0.12$, we estimate $T_c \approx 7$ K. In comparison, the estimated isotropic T_c in MgB_2 is 25–30 K. Enhancement of T_c due to interband anisotropy is expected to be weaker in Li_2B_2 since the two groups of electrons contribute more equally to the coupling with phonons. But even if it were of the same order as in MgB_2 , that is, $\sim 30\%$ in the effective λ , it would only increase T_c to about 15 K. The bottom line is that Li_2B_2 , if synthesized, might be competitive with CaC_6 in terms of T_c , but not with MgB_2 .

However, that is not the end of the story.

While the undoped Li_2B_2 is isoelectronic with MgB_2 , and doping of MgB_2 is known to unequivocally depress T_c , the

same need not be true for Li_2B_2 . Electron doping of MgB_2 lowers the σ DOS, and hence the electron-phonon coupling, since the bands are not ideally 2D. (Though attempts have been made, hole doping of MgB_2 has not yet been achieved.) In Li_2B_2 , the σ bands are much more 2D, so doping should have little effect on their DOS and electron-phonon coupling. On the other hand, electron doping would start filling the π bands, increasing their DOS. Assuming rigid bands, doping on either B or Li sites could be used to raise the Fermi level by nearly 1 eV without losing the contribution from the σ bands. We estimate that this would increase the π -band DOS to roughly half the value in MgB_2 . Doping on the Li sites (with Al, Be, Mg, etc.) should yield even higher π DOS, since the extra ionic charge in the Li planes would lower the π bands relative to the σ bands. Experience shows that it is hard to dope more holes into the σ bands than there already are in pure MgB_2 . Since Li_2B_2 starts with more holes in the σ bands than MgB_2 , it might even be easier to synthesize electron-doped Li_2B_2 than the undoped material. Assuming that the π bands in doped Li_2B_2 couple with the E_{2g} modes at about the same level as in MgB_2 , this additional coupling will soften the E_{2g} phonons and enhance their coupling with the σ bands, without strongly affecting the coupling of ζ bands with soft modes. This is an extremely favorable combination that is likely to have a higher T_c than MgB_2 . To a lesser extent the same holds if the accidental alignment of the Fermi level with the π - π^* crossing is modified by uniaxial pressure.

While Li_2B_2 and related layered lithium borides proposed by Kolmogorov and Curtarolo⁸ are only hypothetical materials as yet, their calculations of the Li-B phase diagram have suggested a route for synthesizing these materials using pressure.⁹ We have shown that, although Li_2B_2 seems to combine the key mechanism for strong electron-phonon coupling in MgB_2 with the dominant coupling mechanism in CaC_6 , each of which has the highest superconducting transition temperature in its respective class of materials, the transition temperature of Li_2B_2 is expected to be lower because of the lack of the seemingly unimportant π electrons at the Fermi level. An appropriately doped version of the material, in which π electrons are restored at the Fermi level, however, could result in a promising new superconductor that combines the paradigms of MgB_2 and CaC_6 in a single material without loss. Further calculations using the virtual crystal approximation or the supercell approximation to explore the quantitative effects of doping on the electron-phonon coupling in this material would be of interest.

ACKNOWLEDGMENTS

We thank L. Boeri, G. Bachelet, and O. K. Andersen for useful discussions, and S. Massida and E. K. U. Gross for sharing with us their work on superconductivity in CaC_6 prior to publication. One of the authors (I.I.M.) thanks Georgetown University for its hospitality during a sabbatical stay. This work was supported by NSF Grant No. DMR-0210717.

- ¹J. M. An and W. E. Pickett, Phys. Rev. Lett. **86**, 4366 (2001).
- ²I. I. Mazin and V. P. Antropov, Physica C **385**, 49 (2003).
- ³W. E. Pickett, cond-mat/0603428 (unpublished).
- ⁴N. Emery, C. Herold, M. d'Astuto, V. Garcia, Ch. Bellin, J. F. Mareche, P. Lagrange, and G. Loupiau, Phys. Rev. Lett. **95**, 087003 (2005).
- ⁵M. Calandra and F. Mauri, Phys. Rev. Lett. **95**, 237002 (2005).
- ⁶I. I. Mazin, L. Boeri, O. V. Dolgov, A. A. Golubov, G. B. Bachelet, M. Giantomassi, and O. K. Andersen, cond-mat/0606404 (unpublished).
- ⁷J. S. Kim, L. Boeri, R. K. Kremer, and F. S. Razavi, Phys. Rev. B **74**, 214513 (2006).
- ⁸A. N. Kolmogorov and S. Curtarolo, Phys. Rev. B **73**, 180501(R) (2006).
- ⁹A. N. Kolmogorov and S. Curtarolo, Phys. Rev. B **74**, 224507 (2006).
- ¹⁰P. Blaha *et al.*, computer code WIEN2K (Karlheinz Schwarz Techn. Universität Wien, Austria, 2001).
- ¹¹J. P. Perdew, K. Burke, and M. Ernzerhof, Phys. Rev. Lett. **77**, 3865 (1996).
- ¹²A. A. Quong and B. M. Klein, Phys. Rev. B **46**, 10734 (1992); A. Y. Liu and A. A. Quong, *ibid.* **53**, R7575 (1996).
- ¹³N. Troullier and J. L. Martins, Phys. Rev. B **43**, 1993 (1991).
- ¹⁴G. Csanyi, P. B. Littlewood, A. H. Nevidomskyy, C. J. Pickard, and B. D. Simons, Nat. Phys. **1**, 42 (2005).
- ¹⁵I. I. Mazin, Phys. Rev. Lett. **95**, 227001 (2005).
- ¹⁶In CaC₆ the ζ band lies substantially lower than in the isoelectronic LiC₃ (cf. Ref. 14). This is due entirely to an additional interlayer compression of the ζ band in LiC₃, due to a smaller c/a [I.I. Mazin (unpublished)].
- ¹⁷Reference 8 reports a 4% enhancement of the anharmonic frequency of the E_{2g} phonon in Li₂B₂ compared to MgB₂, as opposed to our 21% enhancement of the harmonic frequency. The frozen phonon in MgB₂ might indeed be more anharmonic due to the smaller Fermi energy of the σ holes, but anharmonic calculations are known to be exceptionally sensitive to the \mathbf{k} -point sampling. Moreover, it has been shown that the frozen-phonon approach, which includes only one-phonon anharmonic effects, severely overestimates the anharmonicity in MgB₂, and that harmonic calculations are closer to the real frequencies [M. Lazzeri, M. Calandra, and F. Mauri, Phys. Rev. B **68**, 220509(R) (2003)].
- ¹⁸C. O. Rodriguez, A. I. Liechtenstein, I. I. Mazin, O. Jepsen, O. K. Andersen, and M. Methfessel, Phys. Rev. B **42**, 2692 (1990).
- ¹⁹W. L. McMillan, Phys. Rev. **167**, 331 (1968).